

Photometric variability of the unique magnetic white dwarf GD 356

C. S. Brinkworth¹, M. R. Burleigh², G. A. Wynn², T. R. Marsh^{1,3}

¹ Department of Physics and Astronomy, University of Southampton, Highfield, Southampton, UK.

² Department of Physics and Astronomy, University of Leicester, Leicester, LE1 7RH, UK.

³ Department of Physics, The University of Warwick, Coventry, CV4 7AL, UK.

1 November 2018

ABSTRACT

GD 356 is a magnetic white dwarf (B = 13MG) that uniquely displays weak resolved Zeeman triplets of H_α and H_β in emission. As such, GD 356 may be the only known white dwarf with some kind of chromosphere, although accretion from the interstellar medium or more exotic mechanisms cannot be ruled out. Here, we report the detection of low amplitude ($\pm \sim 0.2\%$) near-sinusoidal photometric (V-band) variability in GD 356, with a period of 0.0803 days (~ 115 minutes). We interpret this as the rotation period of the star. We model the variability with a dark spot (by analogy with star spots) covering 10% of the stellar surface. It seems likely that this spot is also the site of the Zeeman emission, requiring the presence of a temperature inversion. We show that the spot is never totally visible or obscured, and that both polar and equatorial spots produce good fits to the data when viewed at high and low inclination respectively.

Key words: Stars: white dwarfs

1 INTRODUCTION

Isolated magnetic white dwarfs are generally recognised by their Zeeman lines of hydrogen or helium in absorption. Studies of local samples of white dwarfs suggest $\sim 10\%$ or more are magnetic in the range $10^4 - 10^9$ G (Liebert, Bergeron & Holberg 2003), and Schmidt et al. (2003) have recently doubled the number of catalogued magnetic white dwarfs to ~ 120 from discoveries in the Sloan Digitised Sky Survey. Many magnetic white dwarfs display surface inhomogeneities, which may be linked to field structure or interstellar accretion, from which their rotation periods can be derived (e.g. RE J0317 – 853, $P_{\text{rot}} \sim 12$ minutes, Barstow et al. 1995). It is notoriously difficult to determine such information for white dwarfs in general, since their absorption lines are significantly broadened by the high surface gravity. Thus, studies of individual magnetic white dwarfs are important for understanding the evolution of the population in general, and the origin of the magnetic sample in particular.

GD 356 (B = 13 MG) is unique among magnetic white dwarfs in showing resolved Zeeman triplets of H_α and H_β in emission (Greenstein & McCarthy 1985). Detailed modelling of spectropolarimetric observations by Ferrario et al. (1997) points to the existence of a latitudinally extended spherical sector or strip covering approximately 10% of the stellar

surface, over which the stellar atmosphere has an inverted temperature distribution at low optical depths. This small region is most likely the site of origin of the emission lines.

The cause of this temperature inversion is a mystery, especially as there is no evidence for a low-mass close, stellar companion. Ferrario et al. (1997) investigated the most obvious interpretation, chromospheric activity, but the evidence for a very localised emission region, and the absence of evidence for such a phenomenon in other similar magnetic white dwarfs argues against such an interpretation. Ferrario et al. (1997) also considered a model invoking Bondi-Hoyle accretion from the interstellar medium, but this interpretation remains unsatisfactory due to a lack of detectable x-ray emission.

Other authors have considered more exotic explanations for the presence of Zeeman-split emission lines in GD 356. For example, Li, Ferrario & Wickramasinghe (1998) suggest that an Earth-like planet, orbiting through the magnetic field with a period of a few hours, might heat the white dwarf's atmosphere near the poles via the generation of electrical currents. Alternatively, and following the work of Zheleznyakov and Serber (1995), Gnedin et al. (2001) propose that in the regions of the magnetic poles cyclotron radiation pressure exceeds the local force of gravity, driving a

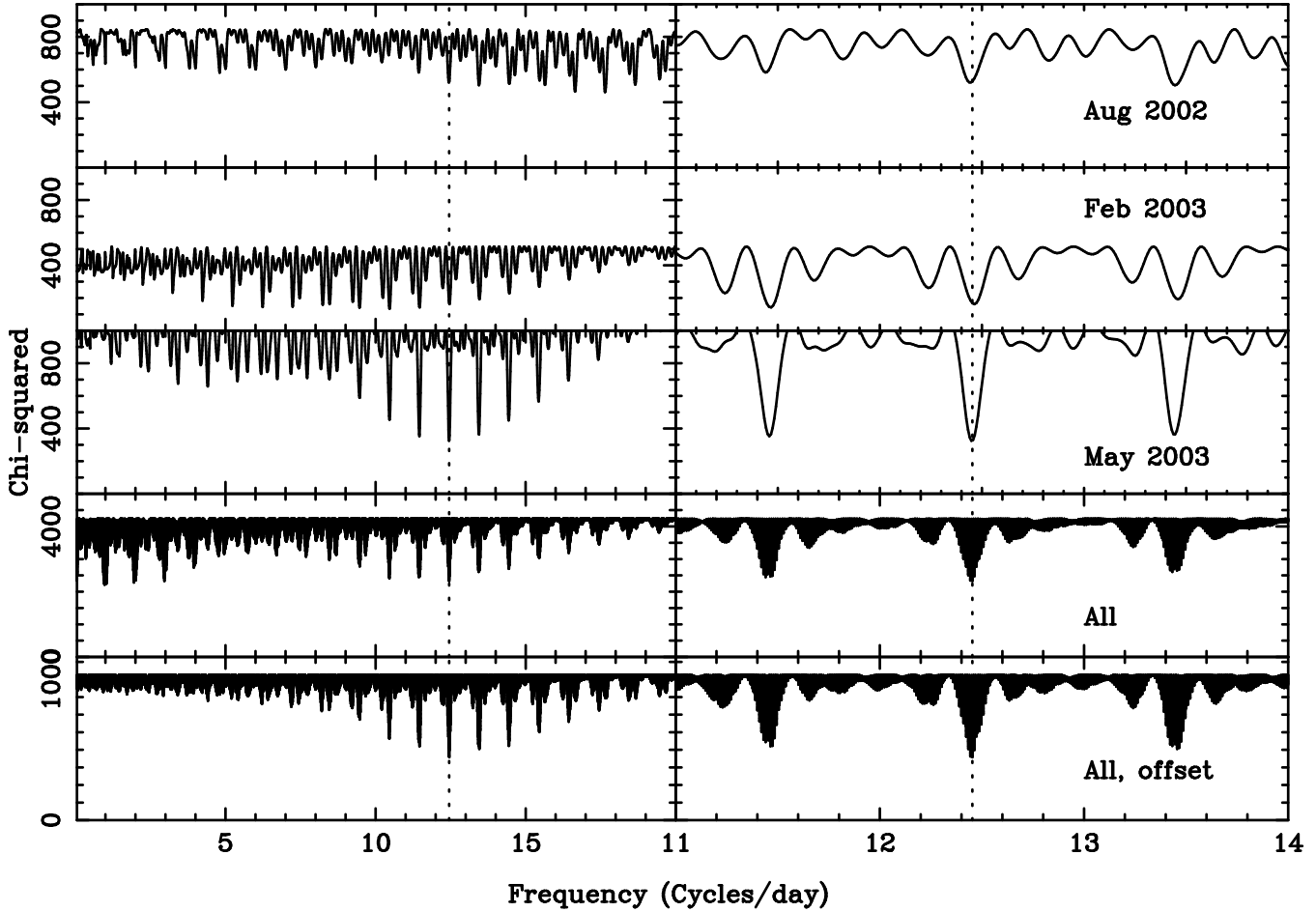


Figure 1. Periodograms for all of the data sets. Panel 1: August 2002. Panel 2: Feb 2003. Panel 3: May 2003. Panel 4: all data. Panel 5: all data, with the average y value of each set offset to zero, removing slight variations in the differential magnitude between each epoch (see Section 3). A period of 0.080300 days is favoured (dotted line).

plasma jet into the magnetosphere. The emission lines may be formed in this outflowing plasma.

Crucially, none of these models were able to utilise information about the rotation period of GD 356, since no evidence for rotation had previously been detected. Ferrario et al.'s multi-epoch spectropolarimetry appeared to rule out rotation in the period range ~ 1 h – 3 year, and a lack of variability in Gnedin et al.'s long-term spectropolarimetric observations led them to conclude that the rotation period of GD 356 exceeds 5 years. Indeed, Ferrario et al. (1997) admit that the details of the star's underlying field geometry are difficult to ascertain with any certainty given the data available to them, especially a lack of rotational modulation.

Here, we present precise V -band photometric observations of GD 356 which reveal low amplitude ($\pm \sim 0.2\%$) near-sinusoidal variability with a period of 0.0803 days (≈ 115 minutes). We argue that this variability is due to rotation, consistent with the presence of a cool, dark spot (analogous to a sunspot) covering a small fraction of the stellar surface. Overlying this region is the temperature inversion at low optical depths, as proposed by Ferrario et al. (1997), which is the site of origin of the emission lines.

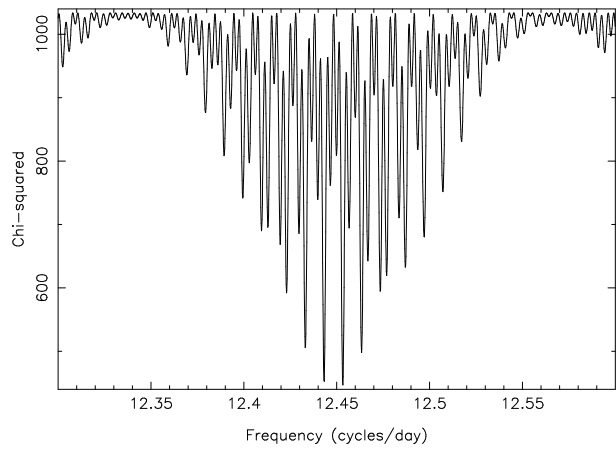


Figure 2. Periodogram zoomed in on the best fitting period of 12.4533 cycles/day.

2 OBSERVATIONS

We observed GD356 at 3 epochs, in August 2002, February 2003 and May 2003 using the 1.0-m Jacobus Kapteyn telescope on La Palma. We used the SITe1 CCD chip, which is

Table 1. List of observations of GD356 taken with the Jacobus Kapteyn Telescope on La Palma.

Date dd/mm/yyyy	Exp (s)	N	Conditions
01/08/02	60	45	Clear, seeing 1.5"
03/08/02	60	10	Clear, seeing 0.7-1"
04/08/02	60	10	Clear, seeing 0.8-1.3"
05/08/02	90	15	Variable. Seeing 0.7-1.5"
06/08/02	60	55	Clear, seeing 0.7"
07/08/02	60	31	Clear, seeing 0.8"
21/02/03	120	34	Clear, seeing 1.4-2"
22/02/03	90	20	Cirrus, seeing 2"
25/02/03	60	27	Clear, seeing 1-1.2"
26/02/03	90	28	Clear, seeing 1.5"
25/05/03	85	66	Clear, seeing 1"
27/05/03	120	50	Clear, seeing 1"
30/05/03	120	40	Clear, seeing 1"
31/05/03	120	50	Clear, seeing 0.8"

2088x2120 pixels, with readout noise = 6 e/ADU and gain = 1.9. The observations were all taken using a V Harris filter with a typical exposure time of 60-90s. The chip was windowed to improve the readout time for the August and May runs, but not for the February run due to reduction software problems at the time. See Table 1 for a full list of observations.

3 DATA REDUCTION

The data were all reduced using TRM's ULTRACAM pipeline software. Bias frames for each night were combined to create a master bias, which was then subtracted from all other frames. Sky flats were then checked, and any with counts of less than 10000 or greater than 35000 were discarded. The remaining flats were combined to create a master flat for each night that was normalised and divided from the target frames. There were no sky flats for the 22nd, 25th or 26th of February so the target frames from those nights were flat-fielded using combined dome flats.

Differential photometry was performed on the target with respect to 2 bright comparison stars in the field. Once we had established that neither was varying, we then used the data that was reduced with respect to the brightest comparison. Results were output in differential magnitudes.

We used a "floating mean" periodogram (e.g. Cumming, Marcy & Butler 1999, Morales-Rueda et al. 2003) to determine the period of each epoch separately, and all of the data together. This is a generalisation of the Lomb-Scargle periodogram (Lomb 1976, Scargle 1982) and involves fitting the data with a sinusoid plus constant of the form:

$$A + B \sin[2\pi f(t - t_0)],$$

where f is the frequency and t is the observation time. The advantage over the Lomb-Scargle periodogram is that it treats the constant, A , as an extra free parameter rather than fixing the zero-point and then fitting a sinusoid, i.e. it allows the zero-point to "float" during the fit. The resultant periodogram is an inverted χ^2 plot of the fit at each frequency. Periodograms of each epoch and all of the data combined can be seen in Fig 1.

There is a small offset in differential magnitude between

each epoch which may be a sign of a second, longer-term, variability, but more data will be required to verify this result. In order to obtain a clearer periodogram for the short-term variation, we removed this long-term variation by offsetting the average y value of each data set to zero, hence the August, February and May data sets were offset in y by -0.208, -0.206 and -0.204 differential mags respectively. The bottom panel of Fig 1 shows the periodogram for all the data when the long-term variation has been removed. As the standard error estimates output by the ULTRACAM software are likely to be an underestimate due to the relatively high signal-to-noise of the data, the error bars for this last data set were re-scaled by adding 0.001 in quadrature to the quoted errors to bring the reduced chi-squared down to 1. This data set was then used to generate the best-fit period and ephemeris.

Two periods were found to be significantly (difference in chi-squared > 60) better than the rest (see Fig 1):

$$HJD = 2452715.07580(5) + 0.0803000(7)E$$

and

$$HJD = 2452715.97555(5) + 0.0803652(3)E$$

where the ephemeris given is the point of minimum light for which the correlation between the fitted zero point and period is at a minimum.

The shorter period is marginally favoured as its chi-squared is 4 less than that of the longer period.

4 A COOL SPOT VARIABILITY MODEL

The analysis of spectropolarimetric observations of GD 356 undertaken by Ferrario et al. (1997) led those authors to conclude that magnetic activity is confined to a limited, latitudinally extended spherical sector or strip which covers around 10% of the stellar surface. The presence of H_α and H_β in emission shows that a temperature inversion exists in this region, but since the gas is tenuous and optically thin it is energetically insignificant and unlikely to contribute to the continuum emission. By analogy with star- and sun-spots, where convective energy flow is suppressed by high magnetic fields (at $T_{eff} \sim 7500$ K, GD 356 has a convective atmosphere, Bergeron, Leggett & Ruiz 2001), we expect regions of higher field such as this to be dark. In this section we aim to show that the near sinusoidal variability visible in our V -band light curve is consistent with this dark spot.

We assume this spot to be a circular area of the stellar surface which subtends an angle β around colatitude θ_m , as measured from the rotation axis of the white dwarf. King and Shaviv (1984) discussed the form of the light curves produced by self occultation of a hot emission region by the white dwarf body. A dark spot can produce quasi-sinusoidal light curves in a similar manner when the spot is never totally visible or obscured. The following conditions on the positions of maximum visibility

$$|i - \theta_m| + \beta > 90^\circ \quad (1)$$

and, minimum visibility

$$i + \theta_m + \beta > 90^\circ \quad (2)$$

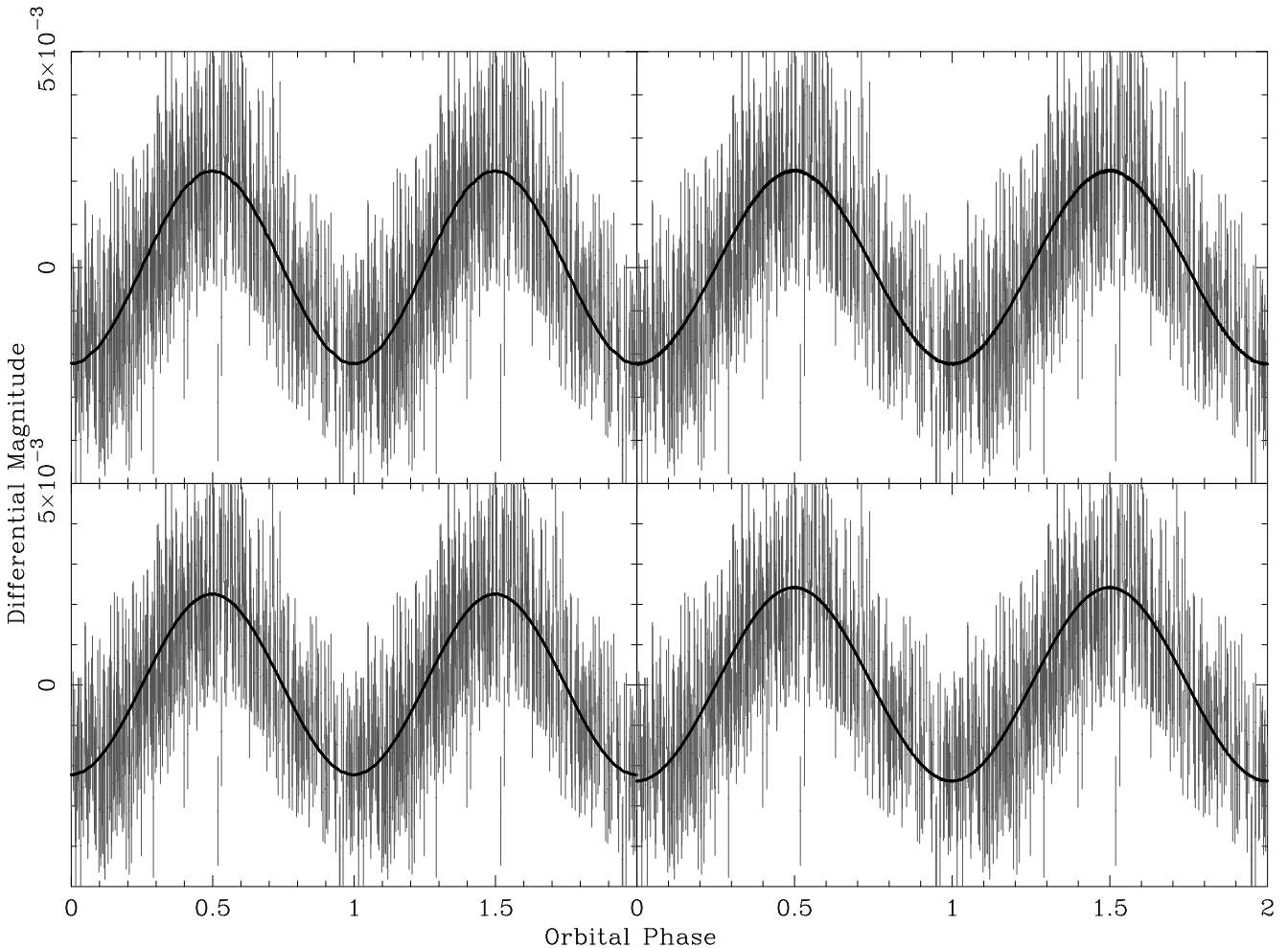


Figure 3. Phase-folded light curve for all data with the slight variations in differential magnitude between each epoch removed (see Section 3). Data is folded on a period of 0.080300 days and fit with 4 different models: top left: $i = 0.7^\circ$, $\theta_m = 60^\circ$, $L_s = 0.1$; bottom left: $i = 1.4^\circ$, $\theta_m = 60^\circ$, $L_s = 0.5$; top right: $i = 60^\circ$, $\theta_m = 0.7^\circ$, $L_s = 0.1$; bottom right: $i = 60^\circ$, $\theta_m = 1.5^\circ$, $L_s = 0.5$. See Section 4 for further details. Vertical bars are errors in differential magnitude, after correction to give a reduced chi-squared of 1 in the periodogram (see Section 3).

of the emission region must be satisfied, where i is the inclination of the observer's line of sight to the stellar rotation axis. For a given β the light curve is a function of the position of the system in the plane $0^\circ \leq i \leq 90^\circ$, $0^\circ \leq \theta_m \leq 90^\circ$. Following the work of Ferrario et al. we fix $\beta = 40^\circ$ giving the region a fractional area of ~ 0.1 . The small amplitude of the variations in the observed light curve of GD 356 ($\pm \sim 0.2\%$) leads to a further constraint on the angles. To produce such small amplitude variations the angular difference between the positions of maximum and minimum visibility (δ) must be small, leading to the constraint

$$|i - \theta_m| - (i + \theta_m) = \delta \rightarrow 0^\circ. \quad (3)$$

Here we have implicitly assumed that the spot is much darker than the surrounding stellar atmosphere. As discussed below this assumption is good if the spot has a relative luminosity compared to the mean global luminosity of the WD $L_s \leq 0.5$. Combining conditions (1), (2) and (3), and using $\beta = 40^\circ$ we find that the inclination angle and the colatitude of the cool region must obey either $(\theta_m > 50^\circ, i \rightarrow 0^\circ)$ or $(i > 50^\circ, \theta_m \rightarrow 0^\circ)$. Hence, within

the assumptions outlined above, we are either observing the rotational modulation of a dark region near the rotational equator from a position near the rotational pole, or conversely, we are observing a spot close to the rotational pole from high inclination.

To investigate the form of the light curve we calculated the visible fraction of the dark spot over a rotational cycle, based on a simple model similar to Wynn and King (1992). The spot was divided into a number (> 100) of equal area sectors with a constant luminosity relative to the surrounding stellar surface. Figure 3 contrasts the data and the model light curves. Both polar and equatorial spots produce a good fit to the data when viewed at high and low inclination respectively. The relative luminosity of the spot makes little difference to the values of i and θ_m required to fit the data for $L_s \leq 0.5$. Of course, there is a large change in the angles required to fit the data as $L_s \rightarrow 1$.

5 DISCUSSION

The low amplitude ($\pm \sim 0.2\%$), 0.0803 day near-sinusoidal photometric (*V*-band) variability of GD 356 is consistent with the rotational modulation of a dark spot covering ($\sim 10\%$), and which is never totally visible or obscured. This spot is either observed near the rotational equator from a position near the rotational pole, or close to the rotational pole from high inclination. The region is presumably the source of the Zeeman-split emission lines of H_α and H_β seen in optical spectra, as proposed previously by Ferrario et al. (1997). Although those authors (and Gnedin et al. 2001) did not report variability of the emission lines, either in velocity or flux, in the light of the discovery of broad-band photometric variability a detection of modulation of the emission lines themselves may provide clues as to their origin. However, this photometric modulation is so small that, even if it is stronger in the Zeeman components than the photometry, it may be difficult to detect. We note that while we have concentrated on the dark-spot model as the source of the photometric variability, we are unable to rule out a grey-spot model (ie a spot which is not cool enough to appear dark, extending over a larger area), or a non-uniform temperature distribution across the surface of the white dwarf, unrelated to the chromospheric spot.

We have deliberately not attempted here to give a physical explanation for the origin of the Zeeman-split emission lines that make GD 356 unique even among the rare magnetic white dwarfs. Chromospheric activity (and an associated x-ray bright corona) is an obvious explanation, but no evidence for such a phenomenon has ever been detected from a magnetic white dwarf (e.g. Arnaud, Zheleznyakov and Trimble 1992, Cavallo, Arnaud and Trimble 1993). From *ROSAT* observations, Muielak, Porter and Davis (1995) give the upper limit on the x-ray luminosity of GD 356 at a few $\times 10^{26}$ erg s $^{-1}$, the same order of magnitude as the luminosity of the solar corona. The only white dwarf that might have a corona detected at x-ray wavelengths, KPD 0005+5106, has an implied luminosity five orders of magnitude higher (Fleming, Werner and Barstow 1993). The evidence for a very localised emission region led Ferrario et al. (1997) to also argue against the chromospheric activity / hot corona interpretation.

Alternatively, GD 356 might be accreting either from a nearby companion or via Bondi-Hoyle accretion from an interstellar medium. However, near-infrared photometry presented by Ferrario et al. (1997) rules out the presence all but very low mass non-stellar companions, and the lack of detectable x-ray emission by Musielak, Porter and Davis (1995) renders the accretion scenario unsatisfactory at present.

We note, though, that new, more sensitive x-ray observations of GD 356 have recently been scheduled with the *Chandra* observatory. The detection of hard x-ray emission, and possibly x-ray variability on the same timescale as the optical oscillations reported here would give credibility to the chromospheric activity and/or accretion models.

6 ACKNOWLEDGEMENTS

CSB acknowledges the support of a PPARC studentship. MRB, GAW and TRM also acknowledge the support of

PPARC. We thank the anonymous referee for helpful comments.

The Jacobus Kapteyn Telescope is operated on the island of La Palma by the Isaac Newton Group in the Spanish Observatorio del Roque de los Muchachos of the Instituto de Astrofisica de Canarias. This research has made use of the SIMBAD database, operated at CDS, Strasbourg, France.

REFERENCES

Arnaud K.A., Zheleznyakov V.V., Trimble V., 1992, PASP, 104, 239
 Barstow M.A., Jordan S., O'Donoghue D., Burleigh M.R., Napiwotzki R., Harrop-Allin M.K., 1995, MNRAS, 277, 971
 Bergeron P., Leggett S.K., Ruiz M.T., 2001, ApJS, 133, 413
 Cavallo R., Arnaud K.A., Trimble V., 1993, JApA, 14, 141
 Cumming A., Marcy G.W., Butler R.P., 1999, ApJ, 526, 890
 Ferrario L., Wickramasinghe D.T., Liebert J., Schmidt G.D., Biegling J.H., 1997, MNRAS, 289, 105
 Fleming T.A., Werner K., Barstow M.A., 1993, ApJ, 416, L79
 Gnedin Y. N., Borisov N.V., Natsvlishvili T.M., Piotrovich M.Y., 2001, Astrophysics, 44, 321
 Greenstein J.L., McCarthy J.K., 1985, ApJ, 289, 732
 King A.R., Shaviv G., 1984, MNRAS, 211, 883
 Li J., Ferrario L., Wickramasinghe D., 1998, ApJ, 503, L151
 Liebert J., Bergeron P., Holberg J.B., 2003, AJ, 125, 348
 Lomb N.R., 1976, Ap&SS, 39, 447
 Morales-Rueda L., Maxted P.F.L., Marsh T.R., North R.C., Heber U., 2003, MNRAS, 338, 752
 Musielak Z.E., Porter J.G., Davis J.M., 1995, ApJ, 453, L33
 Scargle J.D., 1982, ApJ, 263, 835
 Schmidt G.D., et al., 2003, ApJ, in press
 Wynn G.A., King A.R., 1992, MNRAS, 255, 83
 Zheleznyakov V.V., Serber A.V., 1995, Adv. Space Res., 16, 3, 77